Measurement of the Speed and Energy Distribution of Cosmic Ray Muons

Grant Remmen[1, a] and Elwood McCreary[1, b]

[1] *Department of Physics, School of Physics and Astronomy, University of Minnesota, 116 Church Street SE, Minneapolis, MN 55455, USA*

The time of flight distribution of cosmic ray muons was measured for various spacings of detectors filled with plastic scintillator, allowing for a determination of the mean speed, as well as constraint of the energy spectrum below $0.95c$. The use of a time-to-amplitude converter allowed for precise timing measurements and resolution of the shape of the timing distribution for each spacing, necessary for constraining the energy spectrum. The mean speed of cosmic ray muons was found to be $(2.978 \pm 0.007) \times 10^8\,\mathrm{m\,s^{-1}} = (0.993 \pm 0.002)\,c$. The energy spectrum below 0.34 GeV was found to be consistent with a flat distribution and was parameterized with a power law of the form $n(E)\,dE \propto E^{-\alpha} dE$, with α best fit by $(-7.9 \pm 9.1) \times 10^{-4}$.

Keywords: cosmic rays, elementary particles: muons, energy spectrum, relativistic velocity measurement, scintillation detector, nanosecond timing measurement, astroparticle physics, special relativity

I. INTRODUCTION

Cosmic rays, energetic particles from deep space that penetrate Earth's atmosphere, were discovered in 1912 by Victor Hess through the use of a balloon-borne electroscope. Consisting primarily of energetic protons and nuclei produced by supernovae, cosmic rays are constrained by the Galactic magnetic field, forming a relativistic gas with particle energies of up to 10^{21} eV.[6] Upon entering the atmosphere, the primary cosmic rays interact and decay through various other particle species, changing the population from hadrons to leptons, such as muons, which were first detected by cosmic ray physicist Bruno Rossi in 1932.

The very existence of muons at sea level indicates the effects of special relativity. A second generation lepton with properties analogous to the electron, muons have rest mass m_μ of $105.7\,\mathrm{MeV}/c^2$ and rest frame lifetime $\tau \approx 2.2\,\mu$s. Experimental evidence indicates, however, that muons are produced high in the atmosphere, with travel time to sea level much greater than τ in the rest frame of the Earth. The $\sim$ GeV energies of cosmic ray muons at sea level[11] imply speeds greater than $0.999c$, so that relativistic time dilation must be taken into account.

In this experiment, a time-to-amplitude converter (TAC) was used to measure the muon time of flight between detectors, which was on the order of a few ns. This device allowed for more precise measurement of the timing distribution than was obtained in prior measurements of cosmic ray muon speeds at MIT and the University of Minnesota.[2,6] In these prior experiments, the distribution was parameterized by a single speed and was limited in precision ($\sim 10\%$ relative error for Ref. 6). Finally, three scintillator paddles were used for coincidence testing; the use of three paddles decreased the total solid angle over which muon events were collected, which led to greater precision of the measurement. The three-paddle configuration also lessened the probability of independent random background events being incorrectly counted, thereby improving the reliability of the result.

II. THEORY

The special theory of relativity, developed by Einstein over a century ago, governs the behavior of objects moving at relativistic speeds. In particular, Lorentz contraction and time dilation imply that observers will see distances and times in frames in motion relative to them contracted (respectively, lengthened) by factors of $1/\gamma$ and γ, where $\gamma \equiv 1/\sqrt{1-(v/c)^2}$.[10] With relativity taken into account, a muon with $E = 4\,\mathrm{GeV}$ has $\gamma \approx 38$. Hence, the lifetime of the muon, as seen from the Earth, is $\gamma\tau \approx 83\,\mu$s, allowing 4 GeV muons to reach the surface from a height of over 20 km. The observation of the speed of cosmic ray muons, which is close to c, provides an interesting opportunity to observe massive particles in the relativistic limit.

In order to determine the mean speed of cosmic ray muons, a linear fit was calculated. The average time t_{obs} between detections of a muon in paddles separated by a given vertical distance y was measured. This vertical spacing corresponds to an average muon path length l, as not all muons are vertically incident. With l plotted as a function of t_{obs}, the resulting line has slope equal to the mean speed v_μ and the horizontal intercept t_{delay} corresponds to the inherent delay in the detectors and cables:

$$l = v_\mu \left(t_{\mathrm{obs}} - t_{\mathrm{delay}}\right). \tag{1}$$

Cosmic ray muons are not restricted to a single velocity, but are distributed in a spectrum of energies

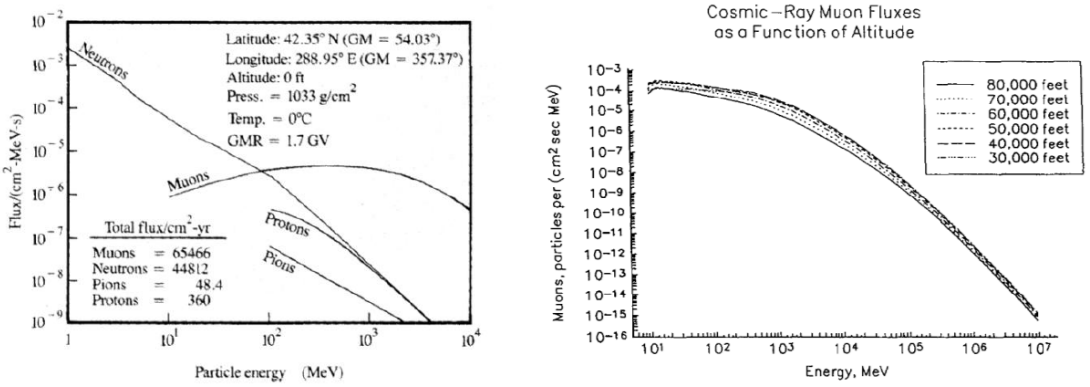

Figure 1: Examples of prediction for various cosmic ray fluxes (figures reproduced from Refs. 12 and 7). Note that the muon distribution does not vary strongly with energy below 1 GeV and is dependent on geographical and atmospheric conditions, such as altitude, location, pressure, etc.

(see Fig. 1). For cosmic ray muons below 1 GeV, the energy spectrum is fairly flat.[4] This statement may be parameterized by a power law:[1]

$$n(E)\,dE \propto E^{-\alpha}dE \implies n(v)\,dv \propto \gamma^{3-\alpha}v dv. \quad (2)$$

The conversion to the velocity distribution follows from the relation $E = \gamma m_\mu c^2$. For a given mean path length l, Eq. (2) may be converted into an expected timing distribution:

$$n(t_{\rm bin})\,\Delta t_{\rm bin} \propto l^2 t_{\rm bin}^{-3}\left(1 - \frac{l^2}{c^2 t_{\rm bin}^2}\right)^{\frac{\alpha-3}{2}} \Delta t_{\rm bin}, \quad (3)$$

where $t_{\rm bin}$ is the time corresponding to a given bin and $\Delta t_{\rm bin}$ is the bin width. By comparing the observed timing distributions with expectations derived from Eq. (3), a fit for the parameter α can be found. In this way, a characterization of the cosmic ray muon velocity distribution allows for constraints to be placed on the energy spectrum.

There exist several sources of uncertainty in the measurement of the mean speed of cosmic ray muons. The angular distribution of cosmic rays follows the empirical relation

$$I = I_0 \cos^n \theta \quad (4)$$

where θ is the zenith angle, I_0 is the flux (counting rate) per unit area per unit solid angle for vertically incident muons, and $n \approx 2$.[5] Angular distribution is a source of uncertainty in measurements of muon speed, due to the variation in possible path lengths. In addition, the variance in path length traversed by signals propagating within the scintillator paddles contributed another source of error in the timing distribution for a given paddle spacing. Other sources of error included electronic jitter and thermal noise in the apparatus. These sources of uncertainty are treated in greater detail in Section IV.

III. EXPERIMENTAL APPARATUS AND METHODS

This experiment involved analyzing the observed time differences between light pulses generated by cosmic ray muons interacting with plastic scintillator material, which was encased in light-tight paddles (see Fig. 2). These pulses were transformed into electrical signals and amplified by photomultiplier tubes (PMTs) to voltages on the order of 10^{2-3} mV. For the scintillator paddles and PMTs used in this experiment, which possess improved sensitivity over those used in Ref. 2, the optimum operating voltages (on the order of -1 kV) had been previously determined. Three scintillator paddles were used, labeled A, B, and C from top to bottom; the perpendicular distance y between paddles A and B was varied among seven different spacings by mounting the paddles on the rungs of a ladder and varying the position of paddle B. For each spacing, data was taken with integration time of approximately 24 hours at a minimum.

The direct signal of a PMT is short in duration, on the order of a few ns, and the shape of the signal pulse is curved, not containing a clean rising or falling edge. In order to produce a longer square pulse more suited to analysis in NIM-standard logic, the signal of each PMT was input into a LeCroy 821 Quad Discriminator. When the PMT voltage exceeds the minimum threshold of 31.5 ± 1.5 mV, the discriminator outputs a square pulse; pulse widths of 64, 24, and 27 ns were used for the outputs of scintillator paddles A, B, and C, respectively. The outputs of the discriminators were used to create in-

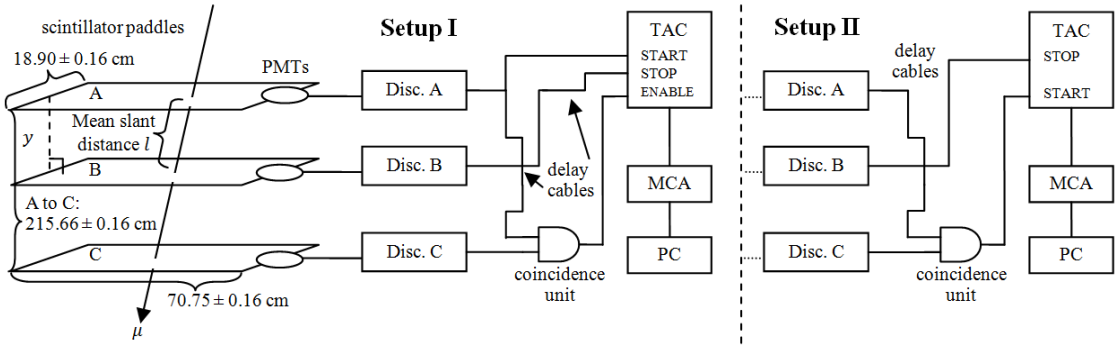

Figure 2: Experimental apparatus for the measurement of the speed of cosmic ray muons, using coincidence Setup I (left) and II (right). Three scintillator paddles (far left) are mounted on a ladder at different spacings. When a muon passes through the paddles, signals from the photomultiplier tubes (PMTs) are re-output by discriminators (Disc.). The time-to-amplitude converter (TAC) measures the interval between events at A and C (plus t_{delay}) and the resulting voltage is input to the multichannel analyzer (MCA) and recorded on a computer (PC).

puts for the START and STOP lines of an ORTEC 566 TAC, which outputs a voltage pulse proportional to the time difference between input pulses. These voltages were then binned and stored using an ORTEC EASY-MCA 1,024-bin multichannel analyzer (MCA), which transferred the data to a computer.

Three-paddle coincidence testing was used both to reduce the probability of a measurement being triggered by independent, unrelated muons and to decrease the relevant solid angle for small y. Complete data sets were taken for two different implementations of the coincidence test (see Fig. 2 for schematics). In Setup I, the clean pulses generated by the discriminators for paddles A and C were input to a C.A.E.N. Model N455 Quad coincidence logic unit (essentially an AND gate), the output of which was sent to the ENABLE line of the TAC. The output from A was sent directly to the START line of the TAC, while the signal from B, delayed by 46 ns using coaxial and LEMO cables, was sent to the STOP line. The signal from paddle A to the AND gate was delayed by a 36 ns coaxial cable, to ensure that it arrived after the signal from C. It was found that Setup I produced significant noise peaks in the timing distribution at high values of y.

In Setup II, which produced less noisy data, the signals from paddles A and C were input into a coincidence gate as before. The signal from A was delayed by a 14 ns LEMO cable, so that, as in Setup I, the signal from A always arrived after C. The coincidence signal was input into the START line of the TAC, with no ENABLE used. The TAC used in this experiment has an inherent limitation on the range of times it can measure: any measurement must be in excess of 10 ns. Therefore, as in Setup I, it was necessary in Setup II to delay the signal from paddle B; in order to accomplish this, B was input to the STOP line with a 36 ns coaxial delay cable. In both Setups I and II, all electronic components were matched at 50 Ω impedance.

As a result of the coincidence tests, this experiment required triple coincidence ($\mathrm{A} \wedge \mathrm{B} \wedge \mathrm{C}$) for a muon to be counted. Following the reasoning of Ref. 8, the expected number of background counts in each bin in our experiment is

$$N_{\mathrm{b}} = 3 n_{\mathrm{A}} n_{\mathrm{B}} n_{\mathrm{C}} T_{\mathrm{tot}} \Delta t_{\mathrm{bin}}^2, \tag{5}$$

where n_{A}, n_{B}, and n_{C} are the count rates in paddles A, B, and C individually (over the solid angle subtended by A and C), T_{tot} is the integration time, and Δt_{bin} is the timing width of a bin (approximately 49 ps). With the total observed background rates of approximately 50 Hz for A and B and 25 Hz for C, $N_{\mathrm{b}} \ll 1$, even for integration times of several days.

The mean path length is dependent on the geometry of the scintillator paddles and the angular distribution of cosmic ray muons, given in Eq. (4). A Monte Carlo simulation was used to calculate the mean path length l for varying y. Pseudorandom coordinates were generated for the location of muon incidence on the top paddle, as well as for the azimuth and zenith angles of the muon's velocity vector. If the muon's trajectory intersected paddles A, B, and C, the muon was ruled successful and l was computed geometrically. After generating 10^5 successful muons for each spacing y between paddles A and B at 1 mm intervals, l was known to a precision on the order of 10^{-6} for a given value of y. Due to the constant solid angle formed by paddles A and C, the relation is well represented by a linear scaling of the perpendicular distance. In Setups I and II, respectively, $(l-y)/y$ was fit as $(9.0001 \pm 0.0007) \times 10^{-3}$ and $(8.9503 \pm 0.0007) \times 10^{-3}$, with the difference be-

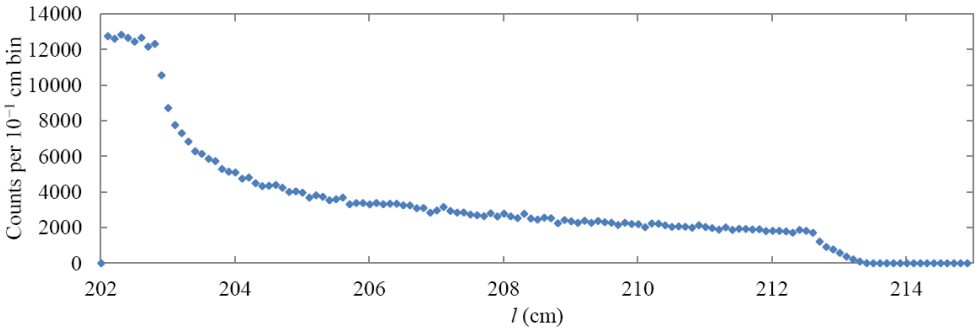

Figure 3: Distribution of accepted lengths from a Monte Carlo simulation of over 4×10^5 muons, with normal spacing y of 202.009375 cm.

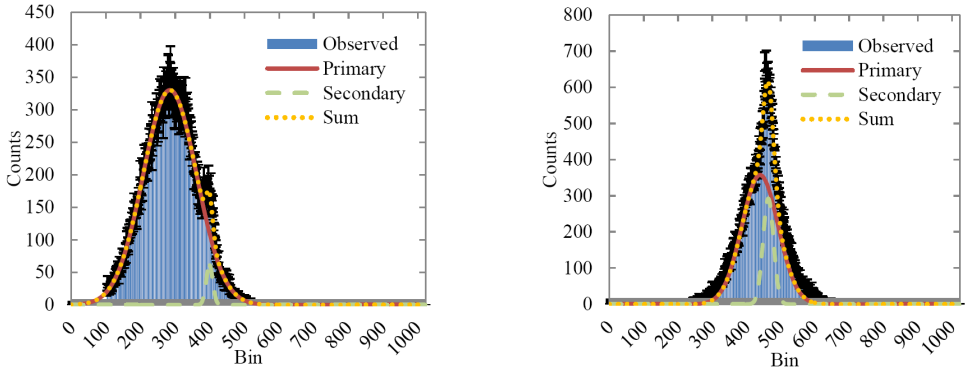

Figure 4: The timing distribution for a mean slant length of 115.80 ± 0.16 and 114.64 ± 0.16 cm for integration times of 48.6 and 50.9 hours, from Data Set I (left) and II (right), respectively. Multiple Gaussian fits for the peak regions of the observed timing distribution (above 20% and 60%, respectively, of the smoothed peak height) are also shown. The reduced χ^2 values for the fits shown are 1.14 and 1.41 for I and II, respectively.

ing due to the 0.64 cm variation between the two Setups of the perpendicular distance between paddles A and C. Though small, in effect lengthening the mean path length by less than 1% over the perpendicular distance y, this correction factor is necessary for an accurate determination of muon speed, given the level of precision in our experiment. A length distribution for a particular y, from a simulation of over 4×10^5 virtual muons, is shown in Fig. 3. Additional Monte Carlo simulations were conducted to assess the effect of misalignment (e.g. paddle B not directly aligned with A and C). It was found that this effect introduces relative errors on the order of 10^{-5} or smaller, which are dwarfed by the 0.16 cm uncertainties in y itself, which was measured directly.

IV. ANALYSIS AND RESULTS

Before the spectrum of speeds (equivalently, energies) could be fit, it was necessary that the inherent delay t_{delay} in the apparatus be found. This was possible by performing a linear fit between the set of mean distances l and the representative times for the respective timing distributions, effectively finding the mean speed of the observed cosmic ray muons. Since the observed timing distributions were non-Gaussian, a multiple (two or three) Gaussian fit was used to parameterize their shapes. In all fits over timing distributions, the error in a particular bin with N counts was taken to be $\sqrt{N}$, by Poisson statistics. Due to the long tails of the distributions, the range of data used for these fits was restricted to the subset with count totals above 20% or 60% of the peak of the distribution for Data Sets I and II, respectively; the eligible regions above the threshold were found by smoothing the data with a local average over five bins. This fitting procedure produced reduced χ^2 values between approximately 1.1 and 2.2 for Data Set I and between 0.8 and 1.4 for Data Set II, indicating fairly good correspondence between the shapes of the timing distributions and those of the fits (see Fig. 4).

For each fit, the peak of the primary Gaussian was taken to correspond to the mean time of flight between paddles A and B for muons passing through the apparatus. For Data Set II, the primary Gaussian corresponds to a shoulder feature near the peak

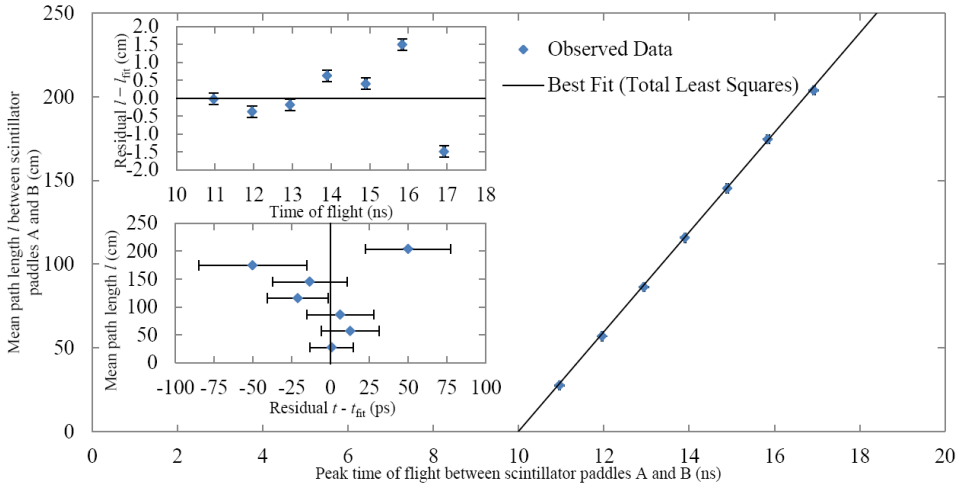

Figure 5: Total least squares linear fit for the mean speed of cosmic ray muons, based on Data Set I. Also shown are the residuals in time and distance, illustrating the quality of the fit, as well as the absence of any obvious systematic trends.

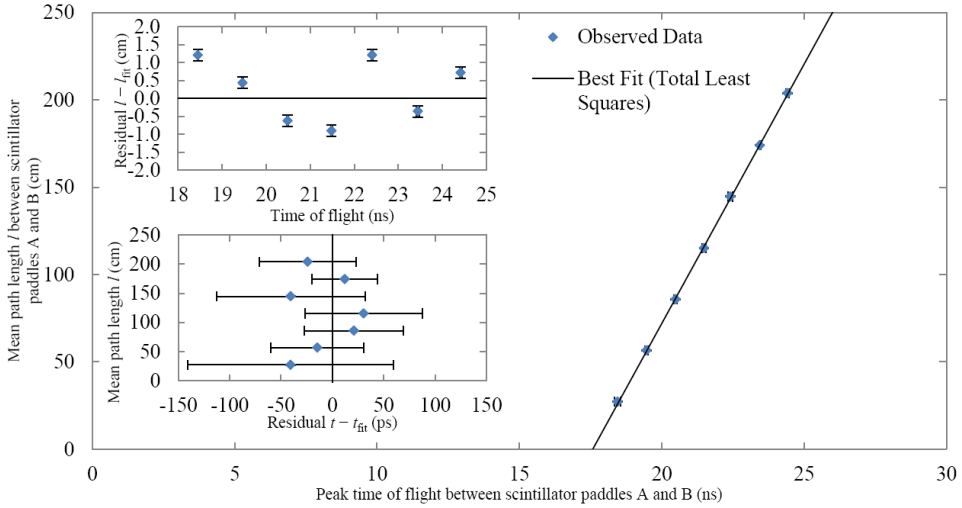

Figure 6: Total least squares linear fit for the mean speed of cosmic ray muons, based on Data Set II. The residuals in time and distance are also plotted, indicating goodness of fit and a lack of clear systematic trends.

(see Fig. 4). In Data Set I, the secondary Gaussian corresponds to a noise peak, possibly due to an internal reflection in the wiring, appearing at nearly the same bin for each spacing. The secondary Gaussian in Data Set II parameterizes the non-Gaussian shape of the distribution, though its origin remains unclear.

The error in the fit time was found using the χ^2+1 method, i.e. varying the mean in both directions until χ^2 is increased by unity. The relative errors in both time and length are on the order of 10^{-3}. Due to the comparable size of the errors in length and time, a linear fit among the seven data points required the implementation of the total least squares method, detailed in Ref. 9. Since this method is not analytically tractable for general errors, the parameters v_μ and t_{delay} were numerically varied until χ^2 was minimized, with the $\chi^2 + 1$ method used for error estimation. For Data Set I, the best fit mean speed was $v_\mu = (2.983 \pm 0.002) \times 10^8\,\text{m}\,\text{s}^{-1} = (0.9950 \pm 0.0006)\,c$ and the timing offset was $t_{\text{delay}} = 10.036 \pm 0.008\,\text{ns}$ (see Fig. 5). For this fit, the reduced χ^2 value was 1.43 for 5 degrees of freedom, at 21% probability. The linear speed fit for Data Set II yielded $v_\mu = (2.969 \pm 0.002) \times 10^8\,\text{m}\,\text{s}^{-1} = (0.9902 \pm 0.0008)\,c$. For configuration II, the timing delay in the apparatus was best fit with $t_{\text{delay}} = 17.57 \pm 0.02\,\text{ns}$ (see Fig. 6). The reduced χ^2 value for

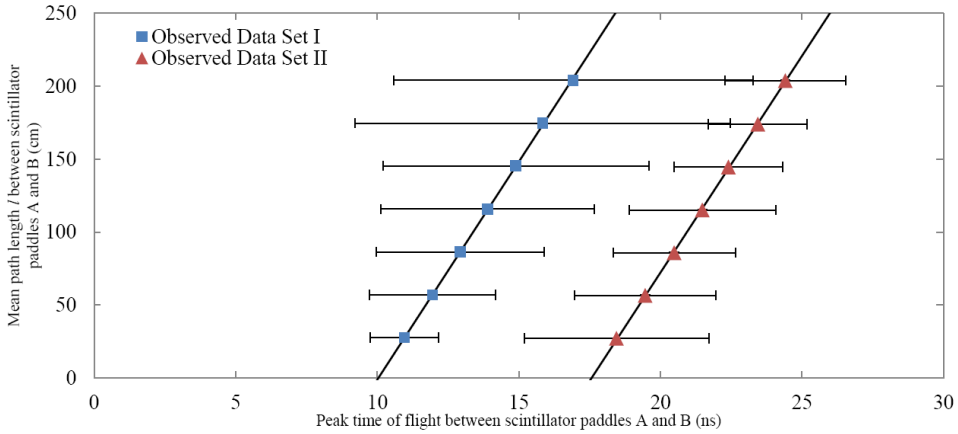

Figure 7: Total least squares linear fit for the speed distribution width of cosmic ray muons, based on Data Sets I and II. The error bars reflect the full widths of the primary Gaussian curves from the multiple Gaussian fits and are overestimates of the true dispersions in the timing distributions caused by velocity variation.

the total least squares fit of Data Set II was 0.29, at 8% probability.

Before calculating the true distribution of velocities, it is instructive to examine what one would obtain for the width of the velocity spectrum, if the errors in the mean time for each spacing are simply taken to be the widths of the Gaussians fit to the timing distributions. Though this method provides an overestimate of the width of the speed distribution, it yields a sense of the tightness of the constraints placed on the distribution by our measurement. In this case, a total least squares fit yields $v_\mu = \left(2.99^{+0.25}_{-0.21}\right)\times 10^8\,\mathrm{m\,s^{-1}} = 0.996^{+0.084}_{-0.072}\times c$ for Data Set I and $v_\mu = \left(2.97^{+0.12}_{-0.11}\right)\times 10^8\,\mathrm{m\,s^{-1}} = 0.991^{+0.039}_{-0.036}\times c$ for Data Set II (see Fig. 7). In this way, our results yield tighter constraints on the speed of cosmic ray muons than other measurements of muon speed in undergraduate laboratories.[2,6]

Finally, the energy spectrum parameter α (see Eq. (2)) can be calculated by an analysis of the shape of the timing distributions. However, the timing distributions observed (as in Fig. 4) are not direct representations of the expected function of Eq. (3). Rather, the timing spectrum in Eq. (3) was convolved (i.e. blurred) with all the sources of error in this experiment. These sources of error included the variance in path length depicted in Fig. 3, as well as thermal noise, jitter in the electronics, variance in the lengths of paths of propagation within the scintillator paddles, and other sources of uncertainty; in effect, these multiple error sources were themselves combined in convolution to give a total effective resolution for our timing distributions.

The total resolution from the combined errors may be parameterized by a Gaussian kernel, though the individual sources are non-Gaussian. The kernel was fit from the timing distributions above a threshold of 25% of the smoothed peak, over bins such that $ct_{\mathrm{bin}} < l$, so that the counts observed in those bins could not correspond to physical particle detections. It is important to note that the method of fitting the Gaussian kernel does not account for systematic errors, such as deviation from expectations of the dependence of muon flux on zenith angle (i.e. $I \propto \cos^n\theta$, with $n \neq 2$) and errors in the tape measure used to determine the perpendicular spacing. The kernels were well fit by Gaussians for Data Set I, with reduced χ^2 values between 0.9 and 1.4; the kernel region of Data Set II was less well fit by Gaussians, with reduced χ^2 ranging from 1.1 to 4.2. For each spacing l, the Gaussian kernel, after being normalized to unit area, was numerically convolved with the distribution given in Eq. (3), with the time for a given bin (t_{obs}) corrected to an absolute time by subtracting t_{delay}. The amplitude of the spectrum was numerically fit for each timing distribution by minimizing χ^2; in this case, analytical fitting of the amplitude was not practicable, due to divergence of the integral of Eq. (3).

The exponent α in the spectrum was fit numerically over all spacings simultaneously by minimizing the total χ^2, with uncertainty found using the χ^2+1 method. In this experiment, α was fit over bins corresponding to muon speeds less than $0.95c$, since the power law exponent is very different at higher energies, where the spectrum is no longer nearly flat. Sample fits for two representative timing distributions are shown in Fig. 8. For Data Set I, it was necessary for the noisy region of the data to be excluded from fitting; the fit for Data Set II appears in good visual agreement with the observed timing distribution.

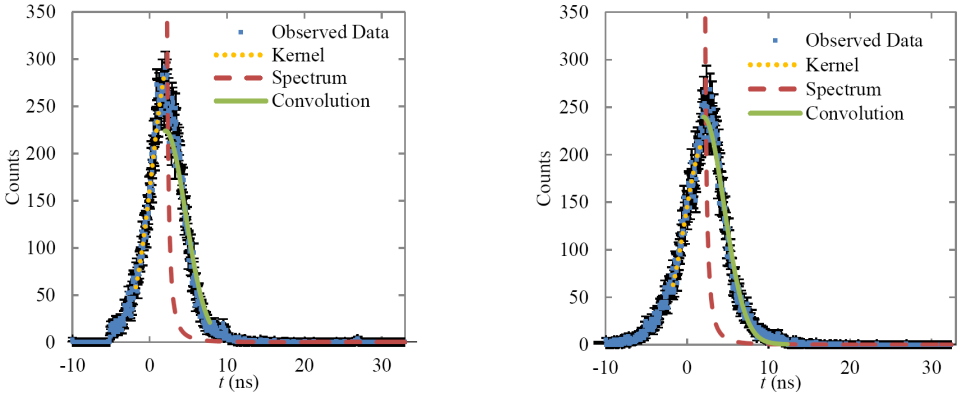

Figure 8: Examples of spectrum fitting for mean slant lengths of $56.94 \pm 0.16\,\mathrm{cm}$ (left) and $56.62 \pm 0.16\,\mathrm{cm}$ (right) for Data Sets I and II, respectively. The observed data are plotted, with t_{bin} corrected by t_{delay}. Also shown are the curves for the Gaussian kernel fitting, the theoretical, noise-free curve from Eq. (3), and the convolution of the pure timing spectrum with the Gaussian resolution.

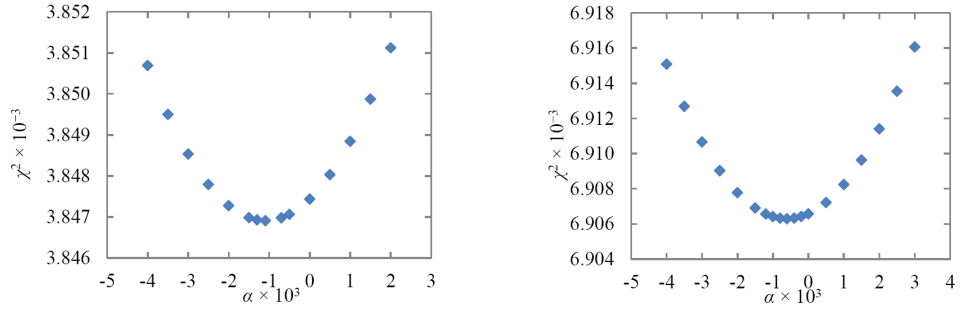

Figure 9: The effect on χ^2 as the energy distribution power law exponent α is varied, for the fit of Data Sets I (left) and II (right). In both cases, the behavior is quadratic, with the minimum at the best fit value of α.

For these fits, the Poisson error in the number of counts in a given bin dominated over the uncertainty in the absolute time. The method used for analyzing the timing distributions assumes that the resolution is the same for fast and slow muons, i.e. that the Gaussian kernel width is constant over the timing distribution. This is the most straightforward *a priori* assumption that allows for the finite resolution of the timing measurement to be taken into account. For Data Set I, the best fit value of α was found to be $(-1.1 \pm 1.5) \times 10^{-3}$, with a reduced χ^2 value of 3.84 over 1,001 degrees of freedom. The fitting process for Data Set II, where the noisy regions of Data Set I did not require exclusion, yielded $\alpha = (-0.6 \pm 1.1) \times 10^{-3}$, for which the reduced χ^2 value was 4.21, with 1,641 degrees of freedom. For both Data Sets, the behavior of χ^2 upon varying α was investigated and found to be quadratic about the best fit value, as expected (see Fig. 9).

V. CONCLUSIONS

In this experiment, the mean speed of cosmic ray muons was measured using two independent implementations of the coincidence test, to a precision of $\sim 10^{-3}$. The χ^2 values for both linear fits were consistent with the number of degrees of freedom. The discrepancy between the mean speeds found from Data Sets I and II was $\Delta v_\mu = (1.4 \pm 0.3) \times 10^6\,\mathrm{m\,s^{-1}} = (4.8 \pm 1.0) \times 10^{-3} c$. The energy loss per unit atmospheric depth,[3] $\sim 2\,\mathrm{MeV\,g^{-1}\,cm^2}$, can only account for approximately $10^3\,\mathrm{m\,s^{-1}}$ of this discrepancy, based on differences in air pressure over Data Sets I and II. The velocity discrepancy was used as an estimate of the systematic uncertainty in our measurement: $\sigma_{v,\mathrm{sys}} = \Delta v_\mu / 2 = 7.1 \times 10^5\,\mathrm{m\,s^{-1}} = 2.4 \times 10^{-3} c$. In the interest of making a conservative estimate of the mean speed, this systematic uncertainty was applied to neither speed individually; instead, a weighted mean was taken over the two values of v_μ, with $\sigma_{v,\mathrm{sys}}$ added in quadrature in the uncertainty. This yielded a best combined value of

$v_\mu = (2.978 \pm 0.007) \times 10^8\,\mathrm{m\,s^{-1}} = (0.993 \pm 0.002)\,c$. In this way, no assumptions were made about which measurement was more reliable (if one Data Set were favored, the best value of v_μ would shift toward the value from that Data Set and the estimated error would be smaller). The best value of v_μ was consistent with an energy of 1 GeV and within approximately 2.6 standard deviations of the velocity (in excess of $0.999c$) corresponding to the mean ground level cosmic ray muon energy of $\sim 4\,\mathrm{GeV}$.[4] Furthermore, muon energy losses within the several floors of building material above our detectors can partially account for the slightly lower observed speed.

The behavior of the energy spectrum below $0.95c$ (0.34 GeV) was parameterized with a power law: $n(E) \propto E^{-\alpha} dE$; the velocity restriction ensures that higher energies were excluded, at which the energy spectrum changes to a different, steep power law. The two Data Sets yielded consistent values of α, with the best value of α calculated from a weighted mean of the two: $(-7.9 \pm 9.1) \times 10^{-4}$. This result is consistent with expectations of a nearly flat distribution Ref. 4, though more specific predictions are not available, due to the dependence of the muon energy spectrum on meteorological and geographic conditions, illustrated in Fig. 1. However, the reduced χ^2 values for the spectrum fitting were high for both Data Sets, with the largest discrepancies near the peak. This possibly implies that, contrary to predictions, the muon spectrum does not follow a single power law over the low energy range or, alternatively, that the timing resolution of our apparatus cannot be parameterized by a single Gaussian, independent of the time interval. In total, the results of this experiment demonstrate overall consistency with expectations regarding the mean speed and energy distribution of cosmic ray muons.

Acknowledgments

The authors are grateful for the advice of Professors Jeremiah Mans and Clem Pryke, as well as helpful conversations with Kurt Wick and Tanner Prestegard, University of Minnesota.

[a] Electronic address: remme024@umn.edu
[b] Electronic address: mccr0132@umn.edu

[1] Aglietta, M. et al. (1998). *Phys. Rev. D 58*(092005).
[2] Ahrens, M. and J. Bubola (2009). Mean velocity of cosmic ray muons. *Methods of Experimental Physics, University of Minnesota*.
[3] Dmitrieva, A., R. Kokoulin, A. Petrukhin, and D. Timashkov (2011). *Astropart. Phys. 34*(401).
[4] Eidelman, S., Particle Data Group, et al. (2004). *Phys. Lett. B 592*(1).
[5] Hall, R., D. Lind, and R. Ristinen (1970). *Am. J. Phys. 38*(1196).
[6] MIT Dept. of Physics (2010). *Lab Guide* (14).
[7] O'Brien, K. and W. Friedberg (1994). Terrestrial cosmic ray intensities. *Environment International 20*(645).
[8] Pearson, B. and D. Jackson (2010). *Am. J. Phys. 78*(491).
[9] Press, W., S. Teukolsky, W. Vetterling, and B. Flannery (1992). *Numerical Recipes in C*. Cambridge: Cambridge University Press.
[10] Rindler, W. (2001). *Relativity: Special, General, and Cosmological*. Oxford: Oxford University Press.
[11] Rossi, B. (1948). *Rev. of Modern Physics 20*(537).
[12] Ziegler, J. (1996). Terrestrial cosmic ray intensities. *IBM J. Res. Dev 40*(19).